Available online at www.sciencedirect.com
SCIENCE DIRECT®
ELSEVIER Applied Mathematics and Computation 160 (2005) 589–606
APPLIED MATHEMATICS AND COMPUTATION
www.elsevier.com/locate/amc

A diffuse-interface model for axisymmetric immiscible two-phase flow

Junseok Kim *

Department of Mathematics, University of California, 103 Multipurpose Science and Technology Building, Irvine, CA 92697, USA

Abstract

A diffuse-interface model is considered for solving axisymmetric immiscible two-phase flow with surface tension. The Navier–Stokes (NS) equations are modified by the addition of a continuum forcing. The interface between the two fluids is considered as the half level set of a mass concentration c, which is governed by the Cahn–Hilliard (CH) equation—a fourth order, degenerate, nonlinear parabolic diffusion equation. In this work, we develop a nonlinear multigrid method to solve the CH equation with degenerate mobility and couple this to a projection method for the incompressible NS equations. The diffuse-interface method can deal with topological transitions such as breakup and coalescence smoothly without ad hoc 'cut and connect' or other artificial procedures. We present results for Rayleigh's capillary instability up to forming satellite drops. The results agree well with the linear stability theory.

Keywords: Rayleigh instability; Pinch-off; Satellite drops; Coalescence; Cahn–Hilliard equation; Nonlinear multigrid method

1. Introduction

Axisymmetric free boundary problems have excellent approximations to a number of important engineering, industrial and biomedical problems such as

* Address: Department of Mathematics, University of California, Irvine, 103 Multipurpose Science and Technology Building, Irvine, CA 92697, USA.
E-mail address: jskim@math.uci.edu (J. Kim).
URL: http://www.math.uci.edu/~jskim/.

0096-3003/$ - see front matter
doi:10.1016/j.amc.2003.11.020

breakup of a liquid column surrounded by another fluid. One of the great difficulties in the study of two immiscible fluid flows is presence of an unknown interface. The interface changes and may undergo severe deformations such as breakup and merging. The diffuse-interface model provides a natural way of treating the topological changes of the interface. The diffuse-interface model is a novel method for capturing the evolution of complex interfaces. To capture evolution of complex interfaces, we will use the Navier–Stokes–Cahn–Hilliard (NSCH) system [7]. In this NSCH model, a mass concentration field $c(\mathbf{x},t)$ is introduced to denote the mass ratio of one of the components in a heterogeneous mixture of two fluids (e.g., m_1/m where m_1 is the mass of fluid 1, and m is the total mass of the binary fluid in a representative volume V). The mass concentration is coupled to the fluid motion through concentration dependent density, viscosity, and surface tension force. And the resulting system couples the Navier–Stokes equations to fourth order, degenerate, nonlinear parabolic diffusion equation of Cahn–Hilliard type for the concentration. A review paper of diffuse-interface model is given by Anderson et al. [8].

The basic idea is similar to a well-known level set method for incompressible two-phase flows [3]. In this method, the level set function $\phi(\mathbf{x},t)$ is defined as follows:

$$\phi(\mathbf{x},t)\begin{cases} > 0, & \text{if } \mathbf{x} \in \text{ fluid 1},\\ = 0, & \text{if } \mathbf{x} \in \Gamma \text{ (the interface between fluids)},\\ < 0, & \text{if } \mathbf{x} \in \text{ fluid 2} \end{cases}$$

and the evolution of ϕ is given by

$$\frac{\partial \phi}{\partial t} + \mathbf{u}\cdot\nabla\phi = 0, \tag{1}$$

where $\mathbf{u}$ is the fluid velocity. Therefore, the interface, Γ, is the zero level set of ϕ. The surface tension force is calculated by ϕ and we want ϕ to be a distance function near the interface. However, under the evolution (1) it will not necessarily remain as such. So, we need to take a reinitialization step [3] to keep ϕ as a distance function near the interface.

In a diffuse-interface method, mass concentration field $c(\mathbf{x},t)$ is governed by the Cahn–Hilliard equation with advection i.e.,

$$\frac{\partial c}{\partial t} + \mathbf{u}\cdot\nabla c = \frac{1}{\rho}\nabla\cdot(M(c)\nabla\mu), \tag{2}$$

where ρ is the density, $M(c)$ is the concentration dependent mobility, and μ is the chemical potential. We capture the interface by the half level set of a continuous concentration function, i.e., Γ, is the half level set of c:

$$\Gamma = \left\{\mathbf{x} | c(\mathbf{x},t) = \frac{1}{2}\right\}.$$

Surface tension force is calculated by c. Like the level set method, we want $c(\mathbf{x}, t)$ to be locally equilibrated. Right-hand side of (2) corresponds to a reinitialization in level set methods. The advantages of this approach are: (1) Topology changes without difficulties; interfaces can either merge or breakup and no extra coding is required. (2) The concentration field c has physical meanings not only on the interface but also in the bulk phases. Therefore, this method can be applied to many physical phase states such as miscible, immiscible, partially miscible, lamellar phases, to name a few. Fig. 1 shows evolution of the randomly oriented lamellar structure of block copolymers under steady shear flow [1]. (3) It can be naturally extended to multicomponent systems (more than two components, e.g., ternary system) and three space dimensions with straightforward manner. Fig. 2 shows time sequence of two droplets leaving interfaces under surface tension forces. This system consists of three immiscible, density matched fluids, i.e., top and bottom fluid (I), middle fluid (II), and two droplets (III) between interfaces. Surface tension between fluid I and III are greater than others.

The paper is organized in the following manner. The governing equation in cylindrical coordinates is introduced in Section 2. The proposed schemes are numerically tested in Section 3. Finally, conclusions are derived in Section 4.

Fig. 1. Evolution of the lamellar structure under shear flow.

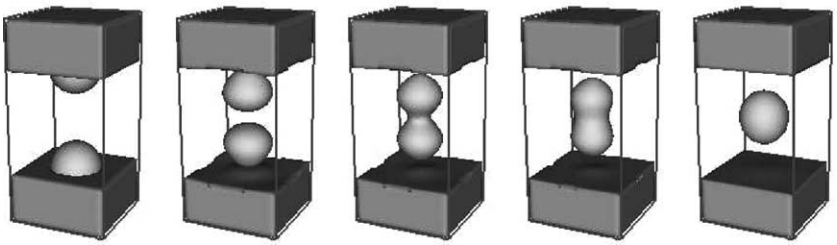

Fig. 2. Evolution of two droplets leaving interfaces under surface tension forces.

2. Numerical method

2.1. Governing equations

We consider a situation of a binary fluid consisting of two components, fluid 1 and fluid 2. We denote the composition of component 1, expressed as a mass fraction, by c. In this setting the composition plays the role of an order parameter that distinguishes the different phases of the fluid. In the present study, we focus our attention on density matched and variable viscosity case here. Therefore, gravity effects are neglected. Let ρ and $\mathbf{u}$ be the density and velocity of the fluid. Then, in dimensional form, the NSCH system [12] is

$$\nabla \cdot \mathbf{u} = 0, \tag{3}$$

$$\rho \dot{\mathbf{u}} = -\nabla p + \nabla \cdot (\eta(c)(\nabla \mathbf{u} + \nabla \mathbf{u}^{\mathrm{T}})) + \sigma \epsilon \alpha \nabla \cdot (|\nabla c|^2 I - \nabla c \otimes \nabla c), \tag{4}$$

$$\rho \dot{c} = \nabla \cdot (M(c) \nabla \mu), \tag{5}$$

$$\mu = f(c) - \epsilon^2 \Delta c, \tag{6}$$

where $\cdot = \partial_t + \mathbf{u} \cdot \nabla$ is the total derivative, ρ is the density, $\mathbf{u}$ is the velocity, p is the pressure, $\eta(c)$ is the viscosity and given by $\eta(c) = \eta_1 c + \eta_2(1-c)$, where η_1 and η_2 are viscosity coefficients of fluid 1 and fluid 2, respectively. $\sigma \epsilon \alpha \nabla \cdot (|\nabla c|^2 I - \nabla c \otimes \nabla c)$ is the interfacial tension body force concentrated on the interface, where I is the identity matrix, σ is the interfacial tension, ϵ is the interface thickness parameter, α is constant, $M(c) = c(1-c)$ is the mobility, μ is the generalized chemical potential, $f(c) = F'(c)$, and $F(c)$ is the Helmholtz free energy. Throughout this paper, $F(c) = \frac{1}{4}c^2(1-c)^2$ is taken.

2.2. Nondimensional governing equations

The next step is to restate the dimensional NSCH system in dimensionless form and for this purpose we define characteristic values such as length (L_*), velocity (V_*), viscosity (η_*), density (ρ_*), chemical potential (μ_*), and mobility (M_*). We then introduce the nondimensional variables for the space coordinates, the velocity components, time, viscosity, the fluid pressure, interface thickness, chemical potential, and mobility as follows:

$$\bar{x} = \frac{x}{L_*}, \quad \bar{\mathbf{u}} = \frac{\mathbf{u}}{V_*}, \quad \bar{t} = \frac{V_* t}{L_*}, \quad \bar{\eta} = \frac{\eta}{\eta_*}, \quad \bar{p} = \frac{p}{\rho_* V_*^2},$$
$$\bar{\epsilon} = \frac{\epsilon}{L_*}, \quad \bar{\mu} = \frac{\mu}{\mu_*}, \quad \bar{M} = \frac{M}{M_*},$$

where the bars denote dimensionless variables. Substituting these variables into the governing equations (3)–(6), dropping the bar notations, and using the dimensionless numbers yields the following nondimensional system:

$$\nabla \cdot \mathbf{u} = 0, \tag{7}$$

$$\mathbf{u}_t + \mathbf{u} \cdot \nabla \mathbf{u} = -\nabla p + \frac{1}{Re} \nabla \cdot [\eta(c)(\nabla \mathbf{u} + \nabla \mathbf{u}^{\mathrm{T}})] + \frac{\epsilon \alpha}{We} \nabla \cdot (|\nabla c|^2 I - \nabla c \otimes \nabla c), \tag{8}$$

$$c_t + \mathbf{u} \cdot \nabla c = \frac{1}{Pe} \nabla \cdot (M(c) \nabla \mu), \tag{9}$$

$$\mu = f(c) - C \Delta c \tag{10}$$

and the dimensionless parameters are Reynolds number, $Re = \rho_* V_* L_* / \eta_*$, Weber number, $We = \rho_* L_* V_*^2 / \sigma$, Cahn number, $C = \epsilon^2 / \mu_*$, and diffusional Peclet number, $Pe = \rho_* L_* V_* / (M_* \mu_*)$.

2.3. The axisymmetric NSCH system

In this paper we consider only axisymmetric flows, therefore there is no flow in the θ (azumusal) direction and all θ derivatives are identically zero. So we consider only two variables; r, the radial direction and z, the axial direction. We define the fluid velocity by the vector $\mathbf{u} = (u, w)$, where $u = u(r, z)$ is the radial component of velocity and $w = w(r, z)$ is the component in the axial direction. The governing equations for axisymmetric flow are

$$\frac{1}{r}(ru)_r + w_z = 0, \tag{11}$$

$$u_t + uu_r + wu_z = -p_r + \frac{1}{Re}\left[\frac{1}{r}(r(2\eta u_r))_r + (\eta(w_r + u_z))_z - \frac{2\eta u}{r^2}\right] + F_1, \tag{12}$$

$$w_t + uw_r + ww_z = -p_z + \frac{1}{Re}\left[\frac{1}{r}(r\eta(w_r + u_z))_r + (2\eta w_z)_z\right] + F_2, \tag{13}$$

$$c_t + uc_r + wc_z = \frac{1}{Pe}\left[\frac{1}{r}(rM(c)\mu_r)_r + (M(c)\mu_z)_z\right], \tag{14}$$

$$\mu = f(c) - C\left[\frac{1}{r}(rc_r)_r + c_{zz}\right], \tag{15}$$

where

$$\mathbf{F} = (F_1, F_2) = \frac{\epsilon \alpha}{We} \nabla \cdot (|\nabla c|^2 I - \nabla c \otimes \nabla c),$$

and

$$\nabla c = (c_r, c_z), \quad \nabla \cdot (\phi, \psi) = \frac{1}{r}(r\phi)_r + \psi_z,$$

where the indexes t, r, and z refer to differentiation with respect to the variable.

2.4. Boundary conditions

We next specify the boundary conditions. Due to the symmetry of the flow, at the column axis ($r = 0$), $u(0,z) = 0$ and $w_r(0,z) = 0$. At the rigid wall, $r = R$, the no-slip conditions are applied, i.e., $u(R,z) = w(R,z) = 0$. For the radial axis we assume periodic boundary conditions, i.e., $\phi(r,0) = \phi(r,H)$, where ϕ is any flow dependent variable and H is the height of the domain. We will denote the domain containing the two fluids as Ω and its boundary as $\partial\Omega$.

2.5. Numerical procedure

Our strategy for solving the system (11)–(15) is a fractional step scheme having two parts: first we solve the momentum and concentration equations (12)–(15) without strictly enforcing the incompressibility constraint (11), then we approximately project the resulting velocity field onto the space of discretely divergence-free vector fields [11].

The computational grid consists of rectangular cells of size Δr and Δz; these cells Ω_{ik} are centered at $(r_i = (i-0.5)\Delta r, z_k = (k-0.5)\Delta z)$, where $i = 1,\ldots,M$ and $k = 1,\ldots,N$. M and N are the number of cells in r-direction and z-direction, respectively. For simplicity, let $h = \Delta r = \Delta z$. The discrete velocity field $\mathbf{u}^n_{ik}$ and concentration field c^n_{ik} are located at cell centers. The pressure $p^{n-\frac{1}{2}}_{i+\frac{1}{2},k+\frac{1}{2}}$ is located at cell corners. The notation $\mathbf{u}^n_{ik}$ is used to represent an approximation to $\mathbf{u}(r_i,z_k,t^n)$, where $t^n = n\Delta t$ and Δt is a time step. Likewise, $p^{n-\frac{1}{2}}_{i+\frac{1}{2},k+\frac{1}{2}}$ is an approximation to $p(r_i+\frac{h}{2}, z_k+\frac{h}{2}, t^n-\frac{\Delta t}{2})$.

The time-stepping procedure is based on the Crank–Nicholson method. At the beginning of each time step, given $\mathbf{u}^{n-1}$, $\mathbf{u}^n$, c^{n-1}, c^n, and $p^{n-\frac{1}{2}}$, we want to find $\mathbf{u}^{n+1}$, c^{n+1}, and $p^{n+\frac{1}{2}}$ which solve the following second-order temporal discretization of the equation of motion:

$$\begin{aligned}\frac{\mathbf{u}^{n+1}-\mathbf{u}^n}{\Delta t} &= -\nabla_d p^{n+\frac{1}{2}} + \frac{1}{2Re}\nabla_d\cdot\eta(c^{n+1})[\nabla_d\mathbf{u}^{n+1} + (\nabla_d\mathbf{u}^{n+1})^{\mathrm{T}}] \\ &\quad + \frac{1}{2Re}\nabla_d\cdot\eta(c^n)[\nabla_d\mathbf{u}^n + (\nabla_d\mathbf{u}^n)^{\mathrm{T}}] + \mathbf{F}^{n+\frac{1}{2}} - (\mathbf{u}\cdot\nabla_d\mathbf{u})^{n+\frac{1}{2}},\end{aligned}$$

$$\frac{c^{n+1}-c^n}{\Delta t} = \frac{1}{Pe}\nabla_d\cdot(M(c^{n+\frac{1}{2}})\nabla_d\mu^{n+\frac{1}{2}}) - (\mathbf{u}\cdot\nabla_d c)^{n+\frac{1}{2}}, \tag{16}$$

$$\mu^{n+\frac{1}{2}} = \frac{1}{2}[f(c^n)+f(c^{n+1})] - \frac{C}{2}\Delta_d(c^n+c^{n+1}), \tag{17}$$

where the updated flow field satisfies the incompressibility condition

$$\nabla_d\cdot\mathbf{u}^{n+1} = 0.$$

The outline of the main procedures in one time step is follows:

Step 1. Initialize c^0 to be the locally equilibrated concentration profile and $\mathbf{u}^0$ to be the divergence-free velocity field.

Step 2. Compute $(\mathbf{u}\cdot\nabla_d c)^{n+\frac{1}{2}}$ by using a second order ENO scheme. In Section 2.5.3 we give a description of how $(\mathbf{u}\cdot\nabla_d c)^{n+\frac{1}{2}}$ is formed.

Step 3. Update the concentration field c^n to c^{n+1}. Details of this step is presented in Section 2.5.1. Once c^{n+1} is obtained, we compute $c^{n+\frac{1}{2}}=\frac{1}{2}(c^n+c^{n+1})$ and $\eta(c^{n+1})$.

Step 4. Compute $(\mathbf{u}\cdot\nabla_d\mathbf{u})^{n+\frac{1}{2}}$ by using a second order ENO scheme and $\mathbf{F}^{n+\frac{1}{2}}$ with $c^{n+\frac{1}{2}}$. In Section 2.5.3 we give a description of how $(\mathbf{u}\cdot\nabla_d\mathbf{u})^{n+\frac{1}{2}}$ is formed. In Section 2.5.2 we give a description of $\mathbf{F}^{n+\frac{1}{2}}$.

Step 5. We solve

$$\frac{\mathbf{u}^*-\mathbf{u}^n}{\Delta t}=-\nabla_d p^{n-\frac{1}{2}}+\frac{1}{2Re}\nabla_d\cdot\eta(c^{n+1})[\nabla_d\mathbf{u}^*+(\nabla_d\mathbf{u}^*)^{\mathrm{T}}]+\frac{1}{2Re}\nabla_d\cdot\eta(c^n)[\nabla_d\mathbf{u}^n+(\nabla_d\mathbf{u}^n)^{\mathrm{T}}]+\mathbf{F}^{n+\frac{1}{2}}-(\mathbf{u}\cdot\nabla_d\mathbf{u})^{n+\frac{1}{2}} \tag{18}$$

using a multigrid method for the intermediate velocity $\mathbf{u}^*$ without strictly enforcing the incompressibility constraint. In Section 2.5.2 we give a description of $\nabla_d p$ and $\nabla_d\cdot\eta(c)[\nabla_d\mathbf{u}+\nabla_d\mathbf{u}^{\mathrm{T}}]$.

Step 6. Project $\mathbf{u}^*$ onto the space of discretely divergence-free vector fields and get the velocity $\mathbf{u}^{n+1}$, i.e., $\mathbf{u}^*=\mathbf{u}^{n+1}+\Delta t\nabla_d\phi$, where ϕ satisfies $\Delta_d\phi=\nabla_d\cdot(\frac{\mathbf{u}^*-\mathbf{u}^n}{\Delta t})$.

Step 7. Update pressure, $p^{n+\frac{1}{2}}=p^{n-\frac{1}{2}}+\phi$.

These complete one time step.

2.5.1. Discretization and numerical solution of the axisymmetric Cahn–Hilliard equation with degenerate mobility

In this section we present a numerical method for the concentration equations (16) and (17). We develop a nonlinear full approximation storage (FAS) multigrid method to solve the nonlinear discrete system at the implicit time level. The nonlinearity is treated using one step of Newton's iteration and a pointwise Gauss–Seidel relaxation scheme is used as the smoother in the multigrid method. See the reference text [6] for additional details and background. Let us rewrite Eqs. (16) and (17) as follows.

$$\mathrm{NSO}(c^{n+1},\mu^{n+\frac{1}{2}})=(\phi^n,\psi^n),$$

where

$$\mathrm{NSO}(c^{n+1},\mu^{n+\frac{1}{2}})=\left(\frac{c^{n+1}}{\Delta t}-\nabla_d\cdot(M_\delta(c)^{n+\frac{1}{2}}\nabla_d\mu^{n+\frac{1}{2}}),\ \mu^{n+\frac{1}{2}}-\frac{1}{2}f(c^{n+1})+\frac{C}{2}\Delta_d c^{n+1}\right)$$

and the source term is

$$(\phi^n, \psi^n) = \left(\frac{c^n}{\Delta t} + s^{n+\frac{1}{2}}, \frac{1}{2} f(c^n) - \frac{C}{2} \Delta_d c^n \right),$$

where $s^{n+\frac{1}{2}} = -(\mathbf{u} \cdot \nabla_d c)^{n+\frac{1}{2}}$. The mobility $M(c)$ is regularized by $M_\delta(c) = \sqrt{c^2(1-c)^2 + \delta}$, where δ is a small positive number (we take $\delta = 10^{-10}$) to avoid any numerical difficulties. In the following description of one FAScycle, we assume a sequence of grids Ω_l (Ω_{l-1} is coarser than Ω_l by factor 2). Given the number v of pre- and post-smoothing relaxation sweeps, an iteration step for the nonlinear multigrid method using the V-cycle is formally written as follows:

FAS multigrid cycle

$$\left\{ c_l^{m+1}, \mu_l^{m+\frac{1}{2}} \right\} = \text{FAScycle}\left(l, c_l^n, c_l^m, \mu_l^{m-\frac{1}{2}}, \text{NSO}_l, \phi_l^n, \psi_l^n, v \right).$$

That is, $\{c_l^m, \mu_l^{m-\frac{1}{2}}\}$ and $\{c_l^{m+1}, \mu_l^{m+\frac{1}{2}}\}$ are the approximations of $c_l(r_i, z_k)$ and $\mu_l(r_i, z_k)$ before and after an FAScycle. Now, define the FAScycle.

(1) Presmoothing: Compute $\{\bar{c}_l^m, \bar{\mu}_l^{m-\frac{1}{2}}\}$ by applying v smoothing steps to $\{c_l^m, \mu_l^{m-\frac{1}{2}}\}$

$$\left\{ \bar{c}_l^m, \bar{\mu}_l^{m-\frac{1}{2}} \right\} = \text{SMOOTH}^v \left(c_l^n, c_l^m, \mu_l^{m-\frac{1}{2}}, \text{NSO}_l, \phi_l^n, \psi_l^n \right),$$

which means performing v smoothing steps with initial approximation $c_l^m, \mu_l^{m-\frac{1}{2}}$, c_l^n, source terms ϕ_l^n, ψ_l^n, and SMOOTH relaxation operator to get the approximation $\bar{c}_l^m$, $\bar{\mu}_l^{m-\frac{1}{2}}$. One SMOOTH relaxation operator step consists of solving the system (21) and (22) given below by 2×2 matrix inversion for each i and k.

Let us discretize Eq. (16) to get a smooth operator.

$$\begin{aligned} \frac{c_{ik}^{n+1}}{\Delta t} + \left(\frac{r_{i+\frac{1}{2}} M_{\delta_{i+\frac{1}{2},k}}^{n+\frac{1}{2}} + r_{i-\frac{1}{2}} M_{\delta_{i-\frac{1}{2},k}}^{n+\frac{1}{2}}}{r_i h^2 Pe} + \frac{M_{\delta_{i,k+\frac{1}{2}}}^{n+\frac{1}{2}} + M_{\delta_{i,k-\frac{1}{2}}}^{n+\frac{1}{2}}}{h^2 Pe} \right) \mu_{ik}^{n+\frac{1}{2}} \\ = \frac{c_{ik}^n}{\Delta t} + s_{ik}^{n+\frac{1}{2}} + \frac{r_{i+\frac{1}{2}} M_{\delta_{i+\frac{1}{2},k}}^{n+\frac{1}{2}} \mu_{i+1,k}^{n+\frac{1}{2}} + r_{i-\frac{1}{2}} M_{\delta_{i-\frac{1}{2},k}}^{n+\frac{1}{2}} \mu_{i-1,k}^{n+\frac{1}{2}}}{r_i h^2 Pe} \\ + \frac{M_{\delta_{i,k+\frac{1}{2}}}^{n+\frac{1}{2}} \mu_{i,k+1}^{n+\frac{1}{2}} + M_{\delta_{i,k-\frac{1}{2}}}^{n+\frac{1}{2}} \mu_{i,k-1}^{n+\frac{1}{2}}}{h^2 Pe}, \end{aligned} \tag{19}$$

where $M^{n+\frac{1}{2}}_{\delta_{i+\frac{1}{2},k}} = M_\delta((c^{n+1}_{ik} + c^{n+1}_{i+1,k} + c^n_{ik} + c^n_{i+1,k})/4)$ and the other values, $M^{n+\frac{1}{2}}_{\delta_{i-\frac{1}{2},k}}$, $M^{n+\frac{1}{2}}_{\delta_{i,k+\frac{1}{2}}}$, and $M^{n+\frac{1}{2}}_{\delta_{i,k-\frac{1}{2}}}$ are calculated similarly.

Next, let us discretize Eq. (17). Since $f(c^{n+1}_{ik})$ is nonlinear with respect to c^{n+1}_{ik}, we linearize $f(c^{n+1}_{ik})$ at c^m_{ik}, i.e.,

$$f(c^{n+1}_{ik}) \approx f(c^m_{ik}) + \frac{\mathrm{d}f(c^m_{ik})}{\mathrm{d}c}(c^{n+1}_{ik} - c^m_{ik}).$$

After substitution of this into (17) and rearranging the terms, we get

$$-\left(\frac{\mathrm{d}f(c^m_{ik})}{2\,\mathrm{d}c} + \frac{2C}{h^2}\right)c^{n+1}_{ik} + \mu^{n+\frac{1}{2}}_{ik} = \frac{1}{2}f(c^n_{ik}) - \frac{C}{2}\Delta_d c^n_{ik} + \frac{1}{2}f(c^m_{ik}) - \frac{\mathrm{d}f(c^m_{ik})}{2\,\mathrm{d}c}c^m_{ik} - \frac{C}{2}\left(\frac{r_{i+\frac{1}{2}}c^m_{i+1,k} + r_{i-\frac{1}{2}}c^{n+1}_{i-1,k}}{r_i h^2} + \frac{c^m_{i,k+1} + c^{n+1}_{i,k-1}}{h^2}\right). \tag{20}$$

Next, we replace c^{n+1}_{jl} and $\mu^{n+\frac{1}{2}}_{jl}$ in Eqs. (19) and (20) with $\bar{c}^m_{jl}$ and $\bar{\mu}^{m-\frac{1}{2}}_{jl}$ if $j \leqslant i$ and $l \leqslant k$, otherwise with c^m_{jl} and $\mu^{m-\frac{1}{2}}_{jl}$, i.e.,

$$\frac{\bar{c}^m_{ik}}{\Delta t} + \left(\frac{r_{i+\frac{1}{2}}M^{n+\frac{1}{2}}_{\delta_{i+\frac{1}{2},k}} + r_{i-\frac{1}{2}}M^{n+\frac{1}{2}}_{\delta_{i-\frac{1}{2},k}}}{r_i h^2 Pe} + \frac{M^{n+\frac{1}{2}}_{\delta_{i,k+\frac{1}{2}}} + M^{n+\frac{1}{2}}_{\delta_{i,k-\frac{1}{2}}}}{h^2 Pe}\right)\bar{\mu}^{m-\frac{1}{2}}_{ik} = \frac{c^n_{ik}}{\Delta t} + s^{n+\frac{1}{2}}_{ik} + \frac{r_{i+\frac{1}{2}}M^{n+\frac{1}{2}}_{\delta_{i+\frac{1}{2},k}}\mu^{m-\frac{1}{2}}_{i+1,k} + r_{i-\frac{1}{2}}M^{n+\frac{1}{2}}_{\delta_{i-\frac{1}{2},k}}\bar{\mu}^{m-\frac{1}{2}}_{i-1,k}}{r_i h^2 Pe} + \frac{M^{n+\frac{1}{2}}_{\delta_{i,k+\frac{1}{2}}}\mu^{m-\frac{1}{2}}_{i,k+1} + M^{n+\frac{1}{2}}_{\delta_{i,k-\frac{1}{2}}}\bar{\mu}^{m-\frac{1}{2}}_{i,k-1}}{h^2 Pe}, \tag{21}$$

$$-\left(\frac{\mathrm{d}f(c^m_{ik})}{2\,\mathrm{d}c} + \frac{2C}{h^2}\right)\bar{c}^m_{ik} + \bar{\mu}^{m-\frac{1}{2}}_{ik} = \frac{1}{2}f(c^n_{ik}) - \frac{C}{2}\Delta_d c^n_{ik} + \frac{1}{2}f(c^m_{ik}) - \frac{\mathrm{d}f(c^m_{ik})}{2\,\mathrm{d}c}c^m_{ik} - \frac{C}{2}\left(\frac{r_{i+\frac{1}{2}}c^m_{i+1,k} + r_{i-\frac{1}{2}}\bar{c}^m_{i-1,k}}{r_i h^2} + \frac{c^m_{i,k+1} + \bar{c}^m_{i,k-1}}{h^2}\right). \tag{22}$$

(2) Compute the defect

$$\left(\bar{d}^m_{1l}, \bar{d}^m_{2l}\right) = \left(\phi^n_l, \psi^n_l\right) - \mathrm{NSO}_l\left(\bar{c}^n_l, \bar{c}^m_l, \bar{\mu}^{m-\frac{1}{2}}_l\right).$$

(3) Restrict the defect and $\left\{\bar{c}^m_l, \bar{\mu}^{m-\frac{1}{2}}_l\right\}$

$$\left(\bar{d}^m_{1l-1}, \bar{d}^m_{2l-1}\right) = I^{l-1}_l\left(\bar{d}^m_{1l}, \bar{d}^m_{2l}\right), \left(\bar{c}^m_{l-1}, \bar{\mu}^{m-\frac{1}{2}}_{l-1}\right) = I^{l-1}_l\left(\bar{c}^m_l, \bar{\mu}^{m-\frac{1}{2}}_l\right).$$

The restriction operator I_l^{l-1} maps l-level functions to $(l-1)$-level functions.

$$\begin{aligned} c_{l-1}(r_i, z_k) = I_l^{l-1} c_l(r_i, z_k) &= \frac{1}{4h^2 r_i} \int_{z_{k-1}}^{z_{k+1}} \int_{r_{i-1}}^{r_{i+1}} c(r,z) r \,\mathrm{d}r \,\mathrm{d}z \\ &= \frac{1}{4h^2 r_i} \left(\int_{z_{k-1}}^{z_k} \int_{r_{i-1}}^{r_i} + \int_{z_{k-1}}^{z_k} \int_{r_i}^{r_{i+1}} + \int_{z_k}^{z_{k+1}} \int_{r_{i-1}}^{r_i} \right. \\ &\quad \left. + \int_{z_k}^{z_{k+1}} \int_{r_i}^{r_{i+1}} c(r,z) r \,\mathrm{d}r \,\mathrm{d}z \right) \\ &= \left[r_{i-\frac{1}{2}} (c_{i-\frac{1}{2},k-\frac{1}{2}} + c_{i-\frac{1}{2},k+\frac{1}{2}}) + r_{i+\frac{1}{2}} (c_{i+\frac{1}{2},k-\frac{1}{2}} + c_{i+\frac{1}{2},k+\frac{1}{2}}) \right] \Big/ (4r_i). \end{aligned}$$

(4) Compute the right-hand side

$$\left(\phi_{l-1}^n, \psi_{l-1}^n\right) = \left(\bar{d}_{1_{l-1}}^m, \bar{d}_{2\,l-1}^m\right) + \mathrm{NSO}_{l-1}\left(\bar{c}_l^n \bar{c}_{l-1}^m, \bar{\mu}_{l-1}^{m-\frac{1}{2}}\right).$$

(5) Compute an approximate solution $\left\{\hat{c}_{l-1}^m, \hat{\mu}_{l-1}^{m-\frac{1}{2}}\right\}$ of the coarse grid equation on Ω_{l-1}, i.e.

$$\mathrm{NSO}_{l-1}\left(c_{l-1}^m, \mu_{l-1}^{m-\frac{1}{2}}\right) = \left(\phi_{l-1}^n, \psi_{l-1}^n\right). \tag{23}$$

If $l = 1$, we explicitly invert a 2×2 matrix to obtain the solution. If $l > 1$, we solve (23) by performing a FAS l-grid cycle using $\left\{\bar{c}_{l-1}^m, \bar{\mu}_{l-1}^{m-\frac{1}{2}}\right\}$ as an initial approximation:

$$\left\{\hat{c}_{l-1}^m, \hat{\mu}_{l-1}^{m-\frac{1}{2}}\right\} = \mathrm{FAScycle}\left(l-1, c_{l-1}^n, \bar{c}_{l-1}^m, \bar{\mu}_{l-1}^{m-\frac{1}{2}}, \mathrm{NSO}_{l-1}, \phi_{l-1}^n, \psi_{l-1}^n, v\right).$$

(6) Compute the coarse grid correction (CGC):

$$\hat{v}_{1l-1}^m = \hat{c}_{l-1}^m - \bar{c}_{l-1}^m, \quad \hat{v}_{2l-1}^{m-\frac{1}{2}} = \hat{\mu}_{l-1}^{m-\frac{1}{2}} - \bar{\mu}_{l-1}^{m-\frac{1}{2}}.$$

(7) Interpolate the correction

$$\hat{v}_{1l}^m = I_{l-1}^l \hat{v}_{1l-1}^m, \quad \hat{v}_{2l}^{m-\frac{1}{2}} = I_{l-1}^l \hat{v}_{2l-1}^{m-\frac{1}{2}}.$$

The interpolation operator I_{l-1}^l maps $(l-1)$-level functions to l-level functions. Then the prolongation operator I_{l-1}^l from Ω_{l-1} to Ω_l is defined by

$$\begin{bmatrix} v_l(r_{i-\frac{1}{2}}, z_{k-\frac{1}{2}}) \\ v_l(r_{i-\frac{1}{2}}, z_{k+\frac{1}{2}}) \\ v_l(r_{i+\frac{1}{2}}, z_{k-\frac{1}{2}}) \\ v_l(r_{i+\frac{1}{2}}, z_{k+\frac{1}{2}}) \end{bmatrix} = \begin{bmatrix} \frac{r_i}{r_{i-\frac{1}{2}}} \\ \frac{r_i}{r_{i-\frac{1}{2}}} \\ \frac{r_i}{r_{i+\frac{1}{2}}} \\ \frac{r_i}{r_{i+\frac{1}{2}}} \end{bmatrix} v_{l-1}(r_i, z_k).$$

(8) Compute the corrected approximation on Ω_l

$$c_l^{m,\text{ after CGC}} = \bar{c}_l^m + \hat{v}_{1l}^m, \quad \mu_l^{m-\frac{1}{2},\text{ after CGC}} = \bar{\mu}_l^{m-\frac{1}{2}} + \hat{v}_{2l}^{m-\frac{1}{2}}.$$

(9) Postsmoothing: Compute $\left\{c_l^{m+1}, \mu_l^{m+\frac{1}{2}}\right\}$ by applying v smoothing steps to $c_l^{m,\text{ after CGC}}$, $\mu_l^{m-\frac{1}{2},\text{ after CGC}}$.

$$\left\{c_l^{m+1}, \mu_l^{m+\frac{1}{2}}\right\} = \text{SMOOTH}^v\left(c_l^n, c_l^{m,\text{ after CGC}},\ \mu_l^{m-\frac{1}{2},\text{ after CGC}},\ \text{NSO}_l, \phi_l^n, \psi_l^n\right).$$

This completes the description of a nonlinear FAScycle.

2.5.2. Discretization of pressure gradient, viscous, and surface tension terms

In this section we describe the axisymmetric finite difference approximation to the pressure gradient ∇p, viscous term $\nabla[\eta(\nabla\mathbf{u} + \nabla\mathbf{u}^{\mathrm{T}})]$, and the surface tension term, $\mathbf{F}$.

$$(\nabla_d p)_{ik} = \begin{pmatrix} \frac{p_{i+\frac{1}{2},k+\frac{1}{2}} + p_{i+\frac{1}{2},k-\frac{1}{2}} - p_{i-\frac{1}{2},k+\frac{1}{2}} - p_{i-\frac{1}{2},k-\frac{1}{2}}}{2h} \\ \frac{p_{i+\frac{1}{2},k+\frac{1}{2}} + p_{i-\frac{1}{2},k+\frac{1}{2}} - p_{i+\frac{1}{2},k-\frac{1}{2}} - p_{i-\frac{1}{2},k-\frac{1}{2}}}{2h} \end{pmatrix}.$$

Let

$$(\mathscr{L}^1, \mathscr{L}^2) = \nabla \cdot \left[\eta\left(\nabla\mathbf{u} + \nabla\mathbf{u}^{\mathrm{T}}\right)\right] = \begin{bmatrix} \frac{2}{r}(r\eta u_r)_r - \frac{2\eta}{r^2}u + (\eta u_z)_z + (\eta w_r)_z \\ \frac{1}{r}(r\eta u_z)_r + \frac{1}{r}(r\eta w_r)_r + 2(\eta w_z)_z \end{bmatrix}.$$

Then the first component of the viscous terms is discretized as follows:

$$\mathscr{L}^1_{ik} = \begin{pmatrix} \frac{2r_{i+\frac{1}{2}}\eta_{i+\frac{1}{2},k}(u_{i+1,k} - u_{ik}) - 2r_{i-\frac{1}{2}}\eta_{i-\frac{1}{2},k}(u_{ik} - u_{i-1,k})}{r_i h^2} \\ -\frac{2\eta_{ik}}{r_i^2}u_{ik} + \frac{\eta_{i,k+\frac{1}{2}}(u_{i,k+1} - u_{ik}) - \eta_{i,k-\frac{1}{2}}(u_{ik} - u_{i,k-1})}{h^2} \\ + \frac{\eta_{i,k+\frac{1}{2}}(w_{i+1,k+1} - w_{i-1,k+1} + w_{i+1,k} - w_{i-1,k})}{4h^2} \\ - \frac{\eta_{i,k-\frac{1}{2}}(w_{i+1,k} - w_{i-1,k} + w_{i+1,k-1} - w_{i-1,k-1})}{4h^2} \end{pmatrix},$$

where $r_{i+\frac{1}{2}} = (r_{i+1} + r_i)/2$, $\eta_{i+\frac{1}{2},k} = [\eta(c_{ik}) + \eta(c_{i+1,k})]/2$, and the other terms are defined similarly.

The second component of the viscous terms, $\mathscr{L}^2_{ik}$, is discretized in a similar manner.

Let the surface tension term

$$\begin{aligned} \mathbf{F} &= -\frac{\epsilon\alpha}{We}(f^1, f^2) = \frac{\epsilon\alpha}{We}\nabla \cdot (|\nabla c|^2 I - \nabla c \otimes \nabla c) \\ &= -\frac{\epsilon\alpha}{We}\left(\frac{1}{r}c_r^2 + c_{zz}c_r - c_z c_{zr}, \frac{1}{r}c_r c_z + c_{rr}c_z - c_r c_{rz}\right). \end{aligned}$$

To match the surface tension of the sharp interface model, α must satisfy

$$\epsilon\alpha\int_{-\infty}^{\infty}(c_z^{\mathrm{eq}})^2\,\mathrm{d}z = 1,$$

where $c^{\mathrm{eq}}(r,z) = [1-\tanh(z/(2\sqrt{2}\epsilon))]/2$ is an equilibrium concentration profile [4]. Then the surface tension term $\mathbf{F}$ is discretized as

$$\begin{aligned} f_{ik}^1 &= \left(\frac{1}{4r_ih^2}(c_{i+1,k}-c_{i-1,k}) + \frac{1}{2h^3}(c_{i,k+1}-2c_{ik}+c_{i,k-1})\right)(c_{i+1,k}-c_{i-1,k}) \\ &\quad - \frac{1}{8h^3}(c_{i,k+1}-c_{i,k-1})(c_{i+1,k+1}+c_{i-1,k-1}-c_{i+1,k-1}-c_{i-1,k+1}), \\ f_{ik}^2 &= \left(\frac{1}{4r_ih^2}(c_{i+1,k}-c_{i-1,k}) + \frac{1}{2h^3}(c_{i+1,k}-2c_{ik}+c_{i-1,k})\right)(c_{i,k+1}-c_{i,k-1}) \\ &\quad - \frac{1}{8h^3}(c_{i+1,k}-c_{i-1,k})(c_{i+1,k+1}+c_{i-1,k-1}-c_{i+1,k-1}-c_{i-1,k+1}). \end{aligned}$$

2.5.3. Approximation of the advection terms

A well-known projection method [11] is used for the flow solver, but we treat the advection terms differently from theirs, where the advection terms are computed using a Godunov procedure. In this section, we describe the discretization of the advection terms. The half time values $\mathbf{u}_{ik}^{n+\frac{1}{2}}$ and $c_{ik}^{n+\frac{1}{2}}$ are calculated using an extrapolation from previous values, i.e., $\mathbf{u}_{ik}^{n+\frac{1}{2}} = \left(3\mathbf{u}_{ik}^{n} - \mathbf{u}_{ik}^{n-1}\right)/2$ and $c_{ik}^{n+\frac{1}{2}} = \left(3c_{ik}^{n} - c_{ik}^{n-1}\right)/2$. From these cell centered values we obtain cell edged values by $\mathbf{u}_{i+\frac{1}{2},k}^{n+\frac{1}{2}} = \left(r_i\mathbf{u}_{ik}^{n+\frac{1}{2}} + r_{i+1}\mathbf{u}_{i+1,k}^{n+\frac{1}{2}}\right)/\left(2r_{i+\frac{1}{2}}\right)$ and $\mathbf{u}_{i,k+\frac{1}{2}}^{n+\frac{1}{2}} = \left(\mathbf{u}_{ik}^{n+\frac{1}{2}} + \mathbf{u}_{i,k+1}^{n+\frac{1}{2}}\right)/2$. In general, the normal velocities $u_{i+\frac{1}{2},k}^{n+\frac{1}{2}}$ and $w_{i,k+\frac{1}{2}}^{n+\frac{1}{2}}$ at the edges are not divergence-free. We apply the MAC projection [9] before constructing the convective derivatives. The equation

$$\Delta_d\phi = \nabla_{\mathrm{MAC}}\cdot\mathbf{u}^{n+\frac{1}{2}} \tag{24}$$

is solved for a cell centered ϕ, where

$$\begin{aligned} \Delta_d\phi_{ik} &= \frac{r_{i+\frac{1}{2}}(\phi_{i+1,k}-\phi_{ik}) - r_{i-\frac{1}{2}}(\phi_{ik}-\phi_{i-1,k})}{r_ih^2} + \frac{\phi_{i,k+1}-2\phi_{ik}+\phi_{i,k-1}}{h^2}, \\ \nabla_{MAC}\cdot\mathbf{u}_{ik}^{n+\frac{1}{2}} &= \frac{r_{i+\frac{1}{2}}u_{i+\frac{1}{2},k}^{n+\frac{1}{2}} - r_{i-\frac{1}{2}}u_{i-\frac{1}{2},k}^{n+\frac{1}{2}}}{r_ih} + \frac{w_{i,k+\frac{1}{2}}^{n+\frac{1}{2}} - w_{i,k-\frac{1}{2}}^{n+\frac{1}{2}}}{h}. \end{aligned}$$

The resulting linear system (24) is solved using a multigrid method, specifically, V-cycles with a Gauss–Seidel relaxation. Then the divergence-free normal velocities $\tilde{u}$ and $\tilde{w}$ are defined by

$$\tilde{u}^{n+\frac{1}{2}}_{i+\frac{1}{2},k} = u^{n+\frac{1}{2}}_{i+\frac{1}{2},k} - \frac{\phi_{i+1,k} - \phi_{ik}}{h}, \quad \tilde{w}^{n+\frac{1}{2}}_{i,k+\frac{1}{2}} = w^{n+\frac{1}{2}}_{i,k+\frac{1}{2}} - \frac{\phi_{i,k+1} - \phi_{ik}}{h}.$$

The convective terms are discretized as:

$$\begin{aligned}(\mathbf{u}\cdot\nabla_d\mathbf{u})^{n+\frac{1}{2}}_{ik} &= \frac{r_{i+\frac{1}{2}}\tilde{u}_{i+\frac{1}{2},k} + r_{i-\frac{1}{2}}\tilde{u}_{i-\frac{1}{2},k}}{2r_i h}\left(\bar{\mathbf{u}}_{i+\frac{1}{2},k} - \bar{\mathbf{u}}_{i-\frac{1}{2},k}\right)\\ &\quad + \frac{\tilde{w}_{i,k+\frac{1}{2}} + \tilde{w}_{i,k-\frac{1}{2}}}{2h}\left(\bar{\mathbf{u}}_{i,k+\frac{1}{2}} - \bar{\mathbf{u}}_{i,k-\frac{1}{2}}\right),\\ (\mathbf{u}\cdot\nabla_d c)^{n+\frac{1}{2}}_{ik} &= \frac{r_{i+\frac{1}{2}}\tilde{u}_{i+\frac{1}{2},k} + r_{i-\frac{1}{2}}\tilde{u}_{i-\frac{1}{2},k}}{2r_i h}\left(\bar{c}_{i+\frac{1}{2},k} - \bar{c}_{i-\frac{1}{2},k}\right)\\ &\quad + \frac{\tilde{w}_{i,k+\frac{1}{2}} + \tilde{w}_{i,k-\frac{1}{2}}}{2h}\left(\bar{c}_{i,k+\frac{1}{2}} - \bar{c}_{i,k-\frac{1}{2}}\right),\end{aligned}$$

where we suppress the $n+\frac{1}{2}$ temporal index. The edge values $\bar{c}^{n+\frac{1}{2}}_{i\pm\frac{1}{2},k}$, $\bar{\mathbf{u}}^{n+\frac{1}{2}}_{i\pm\frac{1}{2},k}$, $\bar{c}^{n+\frac{1}{2}}_{i,k\pm\frac{1}{2}}$, and $\bar{\mathbf{u}}^{n+\frac{1}{2}}_{i,k\pm\frac{1}{2}}$ are computed using a higher order ENO procedure derived in Ref. [5]. The procedure for computing the quantity $f_{i+\frac{1}{2},k}$ is as follows:

$$j = \begin{cases} i & \tilde{u}_{i+\frac{1}{2},k} \geqslant 0,\\ i+1 & \text{otherwise,}\end{cases}$$

$$a = \frac{f_{jk} - f_{j-1,k}}{h}, \quad b = \frac{f_{j+1,k} - f_{jk}}{h}, \quad d = \begin{cases} a & \text{if } |a| \leqslant |b|,\\ b & \text{otherwise,}\end{cases}$$

$$f_{i+\frac{1}{2},k} = f_{jk} + \frac{h}{2}d(1 - 2(j-i)).$$

The quantities $f_{i,k+\frac{1}{2}}$ are computed in a similar manner.

2.5.4. Semi-implicit viscous solve for the intermediate velocity $\mathbf{u}^*$

Let us rewrite Eq. (18)

$$\begin{aligned}&\mathbf{u}^* - \frac{\Delta t}{2Re}\nabla_d\cdot\left[\eta^{n+1}(\nabla_d\mathbf{u}^* + (\nabla_d\mathbf{u}^*)^{\mathrm{T}})\right]\\ &\quad = \mathbf{u}^n - \Delta t\nabla_d p^{n-\frac{1}{2}} - \Delta t(\mathbf{u}\cdot\nabla_d\mathbf{u})^{n+\frac{1}{2}} + \frac{\Delta t}{2Re}\nabla_d\cdot\left[\eta^n(\nabla_d\mathbf{u}^n + (\nabla_d\mathbf{u}^n)^{\mathrm{T}})\right]\\ &\quad\quad + \Delta t\mathbf{F}^{n+\frac{1}{2}}\end{aligned} \tag{25}$$

Let the right-hand side of Eq. (25) be $\mathbf{S}^n$. Then we have

$$\mathbf{u}^* - \frac{\Delta t}{2Re}\nabla_d\cdot\left[\eta^{n+1}\left(\nabla_d\mathbf{u}^* + (\nabla_d\mathbf{u}^*)^{\mathrm{T}}\right)\right] = \mathbf{S}^n = (s_1^n, s_2^n). \tag{26}$$

The first component of Eq. (26) is discretized as follow:

$$\left[1+\frac{\Delta t}{2h^2 Re}\left(\frac{2r_{i+\frac{1}{2}}\eta_{i+\frac{1}{2},k}+2r_{i-\frac{1}{2}}\eta_{i-\frac{1}{2},k}}{r_i}+\frac{2\eta_{ik}h^2}{r_i^2}+\eta_{i,k+\frac{1}{2}}+\eta_{i,k-\frac{1}{2}}\right)\right]u^*_{ik}$$
$$=s^n_{1ik}+\frac{\Delta t}{2h^2 Re}\left[\frac{2r_{i+\frac{1}{2}}\eta_{i+\frac{1}{2},k}u^*_{i+1,k}+2r_{i-\frac{1}{2}}\eta_{i-\frac{1}{2},k}u^*_{i-1,k}}{r_i}+\eta_{i,k+\frac{1}{2}}u^*_{i,k+1}\right.$$
$$+\eta_{i,k-\frac{1}{2}}u^*_{i,k-1}+\frac{\eta_{i,k+\frac{1}{2}}(w^*_{i+1,k+1}-w^*_{i-1,k+1}+w^*_{i+1,k}-w^*_{i-1,k})}{4}$$
$$\left.-\frac{\eta_{i,k-\frac{1}{2}}(w^*_{i+1,k}-w^*_{i-1,k}+w^*_{i+1,k-1}-w^*_{i-1,k-1})}{4}\right]. \tag{27}$$

The second component of Eq. (26) is discretized in a similar manner. The resulting discrete equations are solved using a multigrid method with Gauss–Seidel relaxation.

2.5.5. Discretization of the projection

The result obtained in the last section is a nondivergence-free provisional field $\mathbf{u}^*$. The approximate projection is obtained by solving a Poisson equation for the pressure correction ϕ

$$\Delta\phi=\nabla_d\cdot\left(\frac{\mathbf{u}^*-\mathbf{u}}{\Delta t}\right).$$

Then update new velocity

$$\mathbf{u}^{n+1}=\mathbf{u}^*-\Delta t\nabla\phi$$

and pressure

$$p^{n+\frac{1}{2}}=p^{n-\frac{1}{2}}+\phi.$$

The introduction of this approach to the projection is described in detail in [10] and an axisymmetric discretization is in [9].

3. Numerical result

In this section we apply this method to Rayleigh's capillary instability problems in which surface tension effects and topological changes are present.

3.1. Rayleigh instability

We will consider a long cylindrical thread of a viscous fluid 1, the viscosity and density of which are denoted by η_i and ρ_i respectively, in an infinite mass of

another viscous fluid 2 of viscosity η_o and ρ_o. In the unperturbed state, the interface has a perfectly cylindrical shape with a circular cross-section of radius a. In the thread evolution, the deformation growth rates are consistent with the predictions of the linear stability analysis (e.g. see [13]). In this analysis, the growth of an initially cosinusoidal perturbation to the thread radius a, at leading order, is seen to be given by

$$R(z,t) = a + \alpha(t)\cos(kz),$$

and $\alpha(t) = \alpha_0 e^{int}$, where i$n$ is the growth rate which is a solution of the determinant equation (28) and α_0 is the amplitude of the initial perturbation. In Fig. 3 are shown schematically these parameters. The domain is axisymmetric and the bottom boundary is the axis of symmetry.

$$\begin{vmatrix} I_1(ka) & I_1(k_1'a) & K_1(ka) & K_1(k_1a) \\ kaI_0(ka) & k_1'aI_0(k_1'a) & -kaK_0(ka) & -k_1aK_0(k_1a) \\ 2\beta k^2 I_1(ka) & \beta(k^2+k_1'2)I_1(k_1'a) & 2k^2K_1(ka) & (k^2+k_1^2)K_1(k_1a) \\ F_1 & F_2 & F_3 & F_4 \end{vmatrix} = 0, \tag{28}$$

where

$$F_1 = 2i\beta k^2 I_1'(ka) - \frac{n\rho_i}{\eta_o} I_0(ka) + \frac{\sigma(k^2a^2-1)k}{a^2 n\eta_o} I_1(ka),$$
$$F_2 = 2i\beta k k_1' I_1'(k_1'a) + \frac{\sigma(k^2a^2-1)k}{a^2 n\eta_o} I_1(k_1'a),$$
$$F_3 = 2ik^2 K_1'(ka) + \frac{n\rho}{\eta_o} K_0(ka),$$
$$F_4 = 2ikk_1 K_1'(k_1a),$$

σ is the interfacial surface tension, $\beta = \eta_i/\eta_o$ is the viscosity ratio, $k_1^2 = k^2 + in\rho_o/\eta_o$, $k_1'^2 = k^2 + in\rho_i/\eta_i$, $I_n(x)$ and $K_n(x)$ are the modified Bessel functions of nth order, while $I_n'(x)$ and $K_n'(x)$ denote their first derivatives in respect to x.

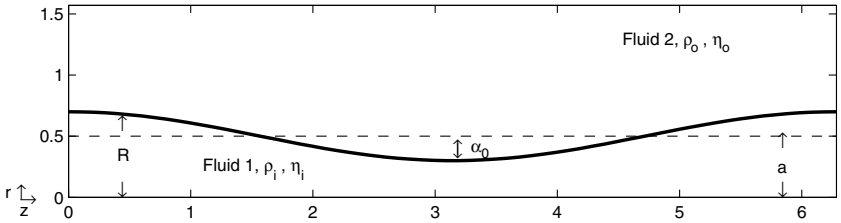

Fig. 3. Schematic of a cylindrical thread of viscous fluid 1 embedded in another viscous fluid 2.

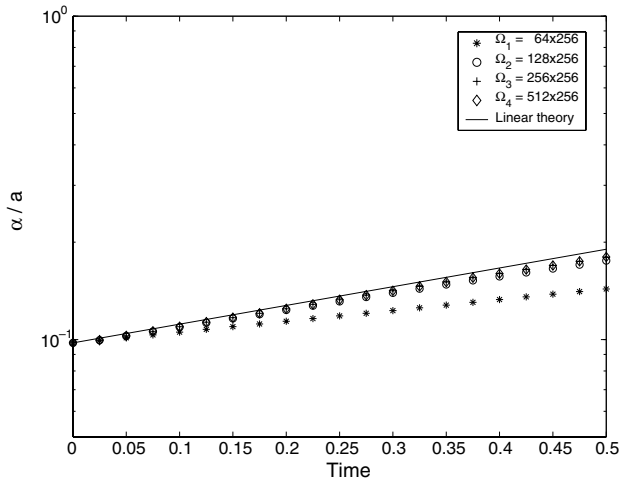

Fig. 4. Evolution of the nondimensional value $\alpha(t)/a$. $\epsilon = 0.02$, $Pe = 100/\epsilon$, $Re = 0.16$, $We = 0.016$. '$*$', 'O', '$+$', and '$\diamondsuit$' are the simulation results on the domains Ω_1, Ω_2, Ω_3, and Ω_4, respectively and the solid line is the linear stability calculation.

Fig. 4 shows evolutions of the nondimensional value $\alpha(t)/a$. The initial concentration field and velocity fields are given by

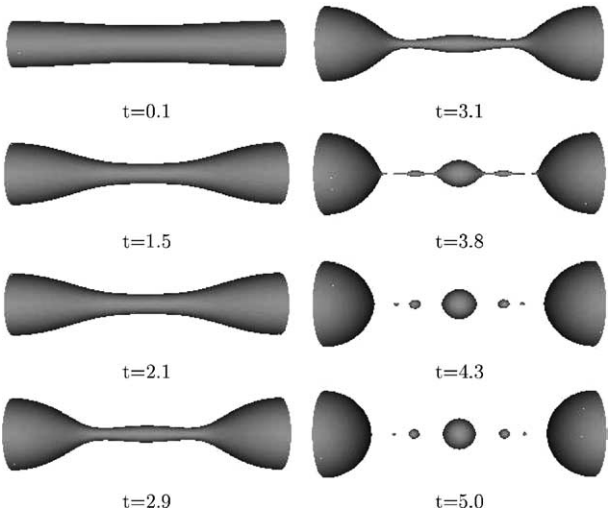

Fig. 5. Time evolution leading to multiple pinch-offs. Viscosity ratio is 0.5, $\epsilon = 0.02$, $Pe = 100/\epsilon$, $Re = 0.16$, and $We = 0.016$. The dimensionless times are shown below each figures.

$$c^0(r,z) = 0.5\left[1 - \tanh\left(\frac{r - 0.5 - 0.05\cos(z)}{2\sqrt{2}\epsilon}\right)\right],$$
$$u^0(r,z) = w^0(r,z) = 0$$

on a domain, $\Omega_n = \{(r,z)|0 \leqslant r \leqslant 2^{n-2}\pi \text{and } 0 \leqslant z \leqslant 2\pi\}$. In this computation we use the parameters: $a = 0.5$, $\alpha(0) = 0.05$, $k = 1$, $\epsilon = 0.02$, $Re = 0.16$, $We = 0.016$, $Pe = 100/\epsilon$, and viscosity ratio $\beta = 1$. '$*$', '$\bigcirc$', '$+$', and '$\diamondsuit$' are the simulation results on the domains Ω_1, Ω_2, Ω_3, and Ω_4, respectively and the solid line is the linear stability calculation. This figure shows that the wall plays no role in the column instability when $n \geqslant 3$. This figure also suggests that the evolution of the disturbances along the early times is well predicted by the linear stability analysis.

An example of the long time evolution of the interface profile is shown in Fig. 5. In the early states ($t = 0.1$, 1.5, and 2.1) the surface contour has only one minimum at exactly $z = \pi$. As the time increases, nonlinearities become important and the initially cosinusoidal shape of the interface changes to a more complex form. The zone of the minimum moves symmetrically off the center ($z = \pi$), giving rise to satellite drops. These satellite drop formations could be attributed to the nonlinear terms in the equations of motion [2].

4. Conclusion

In this paper we have presented a diffuse-interface method for solving axisymmetric immiscible two-phase flow with surface tension. A second-order projection method and a splitting scheme for the concentration field are used to discretize the NSCH system. And resulting discrete equations are solved using multigrid methods. There is no explicit tracking of the fluid interfaces. The fluid interface is recovered at the end of calculation by locating the half level set of a concentration function. We have shown good agreements with the linear stability theory. We also have demonstrated the ability of the diffuse-interface model to compute breakup and merging of the interfaces.

Acknowledgements

The author thanks his advisor, John Lowengrub, for intellectual and financial support. This work was supported by the Department of Energy (Office of Basic Sciences), The National Science Foundation and the Minnesota Supercomputer Institute.

References

[1] H. Kodama, M. Doi, Shear-induced instability of the lamellar phase of a block copolymer, Macromolecules 29 (1996) 2652–2658.
[2] M. Chacha, S. Radeev, L. Tadrist, R. Occelli, Numerical treatment of the instability and breakup of a liquid capillary column in a bounded immiscible phase, Int. J. Multiphase Flow 23 (1997) 377–395.
[3] M. Sussman, E. Fatemi, An efficient, interface-preserving level set redistancing algorithm and its application to interfacial incompressible fluid flow, SIAM J. Sci. Comput. 20 (1999) 1165–1191.
[4] D. Jacqmin, Contact-line dynamics of a diffuse fluid interface, J. Fluid Mech. 402 (2000) 57–88.
[5] C.W. Shu, S. Osher, Efficient implementation of essentially non-oscillatory shock capturing schemes II, J. Comp. Phys. 83 (1989) 32–78.
[6] U. Trottenberg, C. Oosterlee, A. Schüller, MULTIGRID, Academic Press, 2001.
[7] J.S. Lowengrub, L. Truskinovsky, Quasi-incompressible Cahn–Hilliard fluids and topological transitions, Proc. Roy. Soc. Lond. A 454 (1998) 2617–2654.
[8] D.M. Anderson, G.B. McFadden, A.A. Wheeler, Diffuse-interface methods in fluid mechanics, Ann. Rev. Fluid Mech. 30 (1998) 139–165.
[9] M. Sussman, Puckett, G. Elbridge, A coupled level set and volume-of-fluid method for, J. Comput. Phys. 162 (2) (2000) 301–337.
[10] A.S. Almgren, J.B. Bell, W.G. Szymczak, A numerical method for the incompressible Navier–Stokes equations based on an approximate projection, SIAM J. Sci. Comput. 17 (2) (1996) 358–369.
[11] J. Bell, P. Collela, H. Glaz, A second-order projection method for the incompressible Navier–Stokes equations, J. Comp. Phys. 85 (2) (1989) 257–283.
[12] H.Y. Lee, J.S. Lowengrub, J. Goodman, Modeling pinchoff and reconnection in a Hele-Shaw cell. I. The models and their calibration, Phys. Fluids 14 (2) (2002) 492–513.
[13] S. Tomotika, On the instability of a cylindrical thread of a viscous liquid surrounded by another viscous fluid, Proc. Roy. Soc. A 150 (1935) 322–327.